

Magnetic behavior in the $\text{Er}(\text{Mn},\text{Al})_2$ system: Neutron diffraction study

I. V. Golosovsky and A. I. Kurbakov

St. Petersburg Nuclear Physics Institute, 188350, Gatchina, St. Petersburg, Russia

I. Mirebeau

Laboratoire Léon Brillouin, CE-Saclay, 91191 Gif-sur-Yvette, France

A. S. Markosyan and I. Yu. Gaidukova

Faculty of Physics, M. Lomonosov Moscow State University, 119899 Moscow, Russia

(Received 17 July 2003; revised manuscript received 9 September 2003; published 6 November 2003)

A neutron diffraction study of the $\text{Er}(\text{Mn}_{1-x}\text{Al}_x)_2$ system shows that with the substitution of Mn by Al the hexagonal structure of ErMn_2 becomes unstable and is replaced with a cubic structure. In both phases the Mn ions are nonmagnetic or have very small magnetic moments. At $x > 0.02$ a long-range ferromagnetic order observed in ErMn_2 transforms into a canted antiferromagnetic order with induced Mn spins, which, in turn, at $x \geq 0.15$ transforms into a short-range order. In the cubic phase the stability of the antiferromagnetic order is provided by the negative next-nearest-neighbor exchange interaction in the rare-earth lattice, in contrast with other $R(\text{Mn},\text{Al})_2$ systems, where the antiferromagnetic order is stabilized by the strong negative R -Mn interaction. The evaluated ratio of the exchange parameters describing the next-nearest-neighbor and nearest-neighbor Er-Er interactions is found to be $-1/6$.

DOI: 10.1103/PhysRevB.68.184407

PACS number(s): 71.20.Lp, 75.25.+z

I. INTRODUCTION

The intermetallic compounds $R\text{Mn}_2$, where R stands for a rare-earth element, are characterized by a magnetic instability, which is strongly dependent on a certain critical Mn-Mn distance, above which the $3d$ electrons exhibit a localization of the magnetic moment.¹

Our systematic studies of the $\text{Dy}(\text{Mn},\text{Al})_2$ (Ref. 2) and $\text{Ho}(\text{Mn},\text{Al})_2$ (Ref. 3) systems with Mn-Mn distance close to the critical value have revealed a complex magnetic ordering, in which both intrinsic and induced Mn moments coexist. In order to get more insight into the magnetic behavior of the itinerant magnetics $R\text{Mn}_2$ near the region of magnetic instability we have performed a neutron diffraction study of the $\text{Er}(\text{Mn},\text{Al})_2$ system.

In this system the interatomic distances are smaller than in the $\text{Ho}(\text{Mn},\text{Al})_2$ and $\text{Dy}(\text{Mn},\text{Al})_2$ systems and the Mn-Mn spacing is below the critical value. For that reason, in the compound ErMn_2 , Mn ions do not carry magnetic moments.^{4,5} However, the substitution of Mn by Al increases the Mn-Mn spacing, allowing one to reach the instability region from below. The purpose of the present work is an investigation of the magnetic ordering in the $\text{Er}(\text{Mn},\text{Al})_2$ system with increasing Al content.

It is known that $\text{Er}(\text{Mn},\text{Al})_2$ compounds crystallize in the hexagonal structure $C14$ (SG $P6_3/mmc$) and that at small Al content the structure becomes cubic $C15$ (SG $Fd3m$).⁵ It means that it is possible to study the magnetic behavior of compounds with practically identical composition, which differ by the type of packing only, hexagonal or cubic—i.e., by the topology of the magnetic interactions. Note that the edge between the itinerant and localized $3d$ magnetism may be affected by the difference in cubic and hexagonal packing, as was shown for the dimorphic compound $\text{Dy}_{0.8}\text{La}_{0.2}\text{Mn}_2$.⁶

Owing to the variety of complex magnetic structures ob-

served in $R\text{Mn}_2$ compounds, which can coexist in a wide temperature and concentration range, the study of the magnetic properties of substituted systems by macroscopic methods cannot answer many questions. The high-resolution neutron diffraction technique is a very powerful method for this purpose, since it can determine the complex magnetic and atomic order existing in the region of the magnetic instability.

II. EXPERIMENTAL RESULTS

The polycrystalline samples of the $\text{Er}(\text{Mn},\text{Al})_2$ system have been synthesized in an induction furnace in a water-cooled copper crucible. The ingots were subsequently annealed at 750°C for 48 h.

The diffractometer G4-2 of the Laboratory Léon Brillouin with a neutron wavelength of 2.343 \AA was used. All neutron diffraction patterns were treated by the FULLPROF program.⁷ The form factors for Er^{3+} and Mn^{2+} implemented into this program were used.

A. Transformation from hexagonal to cubic structure

The substitution of Mn by Al in $\text{Er}(\text{Mn}_{1-x}\text{Al}_x)_2$ increases the lattice parameter along with the Mn-Mn spacing. In contrast with early neutron diffraction experiments,⁵ where an immediate breakdown of the hexagonal structure was reported, the present experiments show that phases with different structures coexist at low Al concentration. A single cubic phase is observed at $x > 0.25$ only. In Fig. 1 the variation of the cubic and hexagonal fractions is shown as a function of Al concentration.

This result follows immediately from the analysis of the diffraction patterns because there is a set of reflections of the hexagonal phase, which is well separated from the reflections

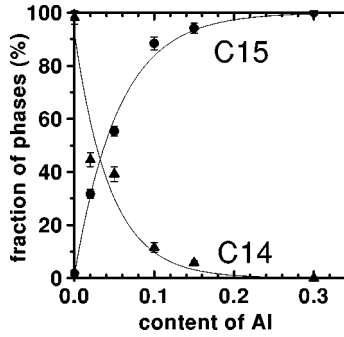


FIG. 1. Fractions of the cubic C15 (solid circles) and the hexagonal C14 phases (solid triangles) at different content of Al. Errors [estimated standard deviation (e.s.d.)] do not exceed the size of the symbols, if not shown. The solid lines are guides for the eye.

of the cubic phase. It gives an opportunity to refine independently with good accuracy not only the structure parameters of two coexisting phases but the size and stress parameters extracted from the peak broadening.

It is known that in the case of an ideal Mn tetrahedra the c/a ratio should be 1.633. However, refinement of the lattice parameters in the hexagonal phase of the substituted compounds shows that the tetrahedra are far from ideal and that they are distorted along the c axis in contrast with ErMn_2 . The edge of the hexagonal prism a increases proportionally with Al content while the height of the prism c goes through a maximum [Fig. 2(a)].

There are two nonequivalent positions $2a$ and $4h$ for Mn(Al) atoms in the hexagonal phase in contrast with the cubic phase. The profile refinement shows that the occupation factors of Al in these nonequivalent positions differ. It explains the uniaxial distortions in the Mn tetrahedra and the observed instability of the hexagonal phase at larger Al content.

In the cubic phase, as well as in the hexagonal one, a marked broadening of the nuclear reflections was observed. The peak broadening due to a size effect is proportional to

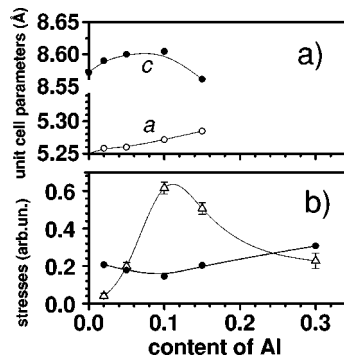


FIG. 2. (a) Concentration dependence of the lattice parameters a (open circles) and c (solid circles) in the hexagonal phase at low temperature. (b) Inner stresses in the cubic phase, which contributes in a Gaussian part of the diffraction profile (triangles) and those in a Lorentz part (solid circles). Errors (e.s.d.) do not exceed the size of the symbols, if not shown. The solid lines are guides for the eye.

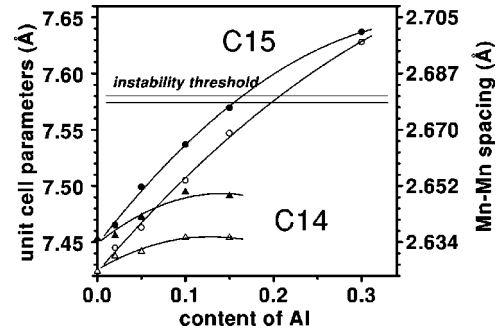


FIG. 3. Concentration dependence of the lattice parameters a and the equivalent parameter a^* for cubic C15 (circles) and hexagonal C14 phases (triangles), respectively, in the $\text{Er}(\text{Mn}_{1-x}\text{Al}_x)_2$ at temperatures 200 K and 2 K (solid and open symbols). The horizontal lines correspond to the critical Mn-Mn distance for the $\text{Ho}(\text{Mn},\text{Al})_2$ and $\text{Dy}(\text{Mn},\text{Al})_2$ systems. Errors (e.s.d.) do not exceed the size of the symbols, if not shown. The solid lines are guides for the eye.

$1/\cos \theta$ (constant in q space), while the broadening due to inner stresses is proportional to $\tan \theta$ ($\sim q$ in q space).

Analysis of the angular dependence of the peak broadening shows that in the hexagonal phase the broadening is mainly due to the size effect, which increases with Al content and is obviously connected with the instability of the hexagonal phase. The minimal averaged size of the particles with hexagonal structure is about 200–250 Å at $x=0.15$.

In contrast with the hexagonal phase, in the cubic phase the broadening of reflections mainly results from inner stresses [Fig. 2(b)]. Surprisingly the variation of the distortions in the hexagonal structure with Al content correlates with the variations of the inner stresses in the cubic phase. It reflects the mutual mechanical interaction of the two coexisting phases.

B. Magnetic behavior of the $\text{Er}(\text{Mn},\text{Al})_2$ system

In Fig. 3 the lattice parameter a of the cubic structure and the equivalent parameter in the hexagonal structure, $a^* = (\sqrt{3}a^2c)^{1/3} = V^{1/3}$, where V is the unit cell volume, are given as a function of Al concentration at two temperatures 200 K and 2 K. The upper and low horizontal lines in Fig. 3 correspond to the lattice parameters at which the critical Mn-Mn distances are reached in the $\text{Ho}(\text{Mn},\text{Al})_2$ (Ref. 3) and $\text{Dy}(\text{Mn},\text{Al})_2$ (Ref. 2) systems, respectively.

In the hexagonal C14 phase the Mn-Mn distances are far below the critical one, so that the Mn intrinsic magnetic moment cannot be stabilized and this phase shows a simple ferromagnetic structure [Fig. 4(a)] with weak Mn moments slightly above three standard deviations.

In ErMn_2 the Er moment is found to be $7.76(4)\mu_B$, close to the values previously reported.^{4,5} The Er moment is oriented along the c axis, in contrast with hexagonal HoMn_2 , where the Ho moments lie in the basal plane.⁸ With increasing Al content the Er moment value shows a minimum at Al concentration at which the maximum of the hexagonal prism height c [Fig. 2(a)] is observed. In contrast with the hexago-

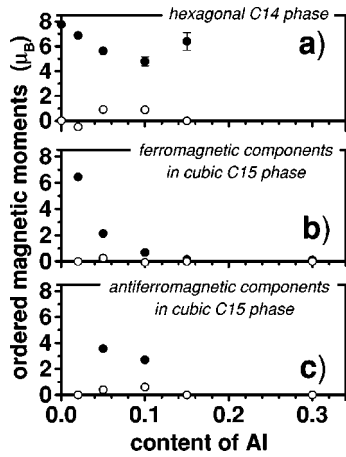


FIG. 4. Magnetic moments of Er (solid circles) and Mn (open circles) vs Al content: (a) in the hexagonal $C14$ phase, (b) ferromagnetic components in the cubic $C15$ phase, and (c) antiferromagnetic components in the cubic $C15$ phase. Errors (e.s.d.) do not exceed the size of the symbols.

nal compound $\text{Dy}_{0.8}\text{La}_{0.2}\text{Mn}_2$,⁶ the magnetic structure is not affected by distortions of the Mn tetrahedra.

In the cubic $C15$ phase the Mn-Mn distance is larger and increases with increasing Al content (Fig. 3), encompassing the instability threshold. Nevertheless, at any Al content the ordered Mn moments are practically absent and Er magnetism dominates. In this phase, the magnetic structure evolves with increasing Al content from ferromagnetic to a canted antiferromagnetic structure, then to a short-range-ordered structure. The ordered ferromagnetic component of the Er moments decreases to zero at Al content $x \sim 0.15$ while a ferromagnetic component of the Mn spins is absent at all x [Fig. 4(b)].

At $x > 0.05$, small antiferromagnetic reflections are detected in the low-temperature diffraction patterns (Fig. 5). They can be indexed with the propagation vector $\mathbf{k} = (\frac{1}{2} \frac{1}{2} \frac{1}{2})$, which corresponds to the second type of antiferro-

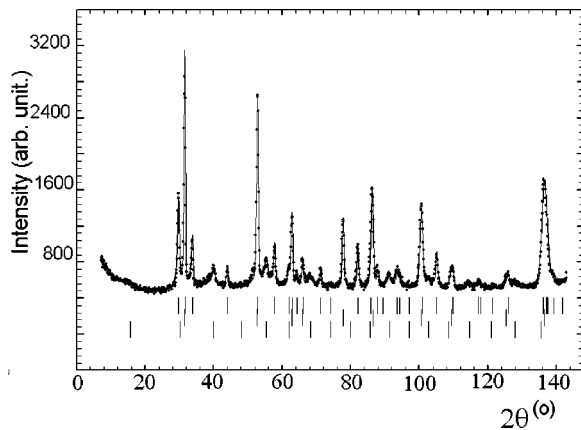


FIG. 5. Neutron diffraction pattern of $\text{Er}(\text{Mn}_{0.95}\text{Al}_{0.05})_2$ measured at 2 K. Upper, middle, and bottom rows of stripes correspond to reflections of the hexagonal, cubic ferromagnetic, and cubic antiferromagnetic structures, respectively.

magnetic ordering in the fcc lattice. The absence of the reflection $\frac{1}{2} \frac{1}{2} \frac{1}{2}$ indicates that the antiferromagnetic components are aligned along the $[111]$ direction. The observed antiferromagnetic reflections are notably broadened, which corresponds to a finite correlation length of about $85(5)$ Å.

The presence of ferromagnetic and antiferromagnetic components in the cubic phase of the $\text{Er}(\text{Mn},\text{Al})_2$ system indicates so-called “canted” (AF2) magnetic structure. This structure is similar to those reported for other cubic RMn_2 compounds: HoMn_2 (Ref. 9), DyMn_2 (Ref. 10) and TbMn_2 (Ref. 11). It is characterized by the existence of nonmagnetic layers of Mn ions inserted between two double ferromagnetic layers with opposite antiferromagnetic components. Such an arrangement, known as a “sandwich”-type structure, is typical of cubic Laves phases in the region of instability.

At high Al content, above $x = 0.15$, a long-range order in the $\text{Er}(\text{Mn}_{1-x}\text{Al}_x)_2$ system disappears and only diffuse magnetic scattering is observed in the difference patterns, showing the presence of a short-range order. This diffuse scattering is maximal around the node $\frac{1}{2} \frac{1}{2} \frac{1}{2}$, corresponding to short-range antiferromagnetic correlations.

At the highest Al content $x = 0.3$, above the instability threshold, one could speculate the presence of disordered intrinsic Mn moments. Several indirect arguments support this interpretation. First, in contrast with the hexagonal phase, where the Er moment weakly depends on Al content, in the cubic phase the ordered ferromagnetic component of the Er moment rapidly decreases [Fig. 4(b)]. A similar rapid reduction of the rare-earth magnetic moment with increasing Al content was observed in $\text{Ho}(\text{Mn},\text{Al})_2$ (Refs. 1 and 3) and $\text{Dy}(\text{Mn},\text{Al})_2$ (Ref. 2) and was attributed to random molecular fields from spontaneous Mn moments.¹ In $\text{Er}(\text{Mn},\text{Al})_2$, the rate of moment reduction is smaller than in $\text{Ho}(\text{Mn},\text{Al})_2$ and $\text{Dy}(\text{Mn},\text{Al})_2$, suggesting smaller values for the disordered intrinsic Mn moments.

Second, the intensity of the diffuse magnetic maxima, which appear at $x \geq 0.1$, increases with increasing Al content, like in Ho and Dy systems. This proposes that the short-range correlations involve intrinsic Mn moments, gradually stabilized by the lattice expansion.

Third, in Fig. 3 it is seen that at the highest Al content the lattice thermal expansion markedly slows down, which is typical for the onset of intrinsic moments. All these facts strongly suggest the appearance of weak spontaneous disordered Mn moments above $x \geq 0.15-0.2$.

III. MAGNETIC INTERACTIONS IN THE CUBIC PHASE

The transformation of the magnetic structure in the cubic phase of the $\text{Er}(\text{Mn},\text{Al})_2$ system from a ferromagnetic to a canted antiferromagnetic one with increasing Mn-Mn spacing differs from that observed in the $\text{Dy}(\text{Mn},\text{Al})_2$ (Ref. 2), $(\text{Dy},\text{Y})\text{Mn}_2$ (Ref. 12), and $(\text{Ho},\text{Y})\text{Mn}_2$ (Ref. 13) systems where a canted antiferromagnetic structure transforms into a collinear antiferromagnetic structure.

The stability of a canted antiferromagnetic phase in DyMn_2 , HoMn_2 , and other Mn-based compounds is provided by the strong negative R -Mn interaction, 4–5 times

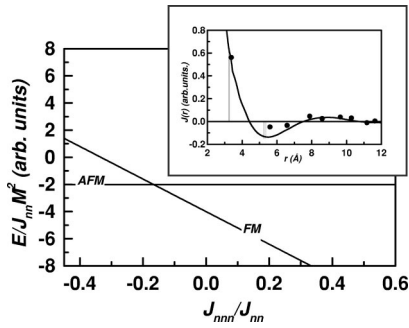


FIG. 6. Variation of the free energy as a function of the exchange parameters ratio J_{nnn}/J_{nn} for antiferromagnetic and ferromagnetic states. In the inset the dependence of RKKY interactions $J(r)$ for NdAl_2 (Ref. 14). Solid circles are the experimental data and the solid line is the least-squares fit. The two pairs of closely placed vertical lines correspond to the radii in the first and second coordination spheres for Al content $0.02 \leq x \leq 0.1$.

larger than the positive R - R interaction.² This interaction is responsible for the transformation of a canted antiferromagnetic structure to a collinear antiferromagnetic structure. A simple model taking into account the nearest-neighbor R - R and R -Mn exchange interactions explains such a transformation.²

In the $\text{Er}(\text{Mn},\text{Al})_2$ system the Mn ions are practically nonmagnetic and R -Mn interactions are negligible. Therefore the model based on the strong negative R -Mn interaction cannot account for the stability of the antiferromagnetic structure observed in the $\text{Er}(\text{Mn},\text{Al})_2$ system in the interval $0.05 \leq x \leq 0.1$.

The stability of the antiferromagnetic structure in the rare-earth lattice with cubic Laves phase structure can be qualitatively explained by taking into account the next-nearest-neighbor exchange interaction J_{nnn} between R ions together with the nearest-neighbor interaction J_{nn} .

The canted antiferromagnetic structure AF2 has been displayed in a number of works, for example, in Fig. 6 of Ref. 2. In this type of ordering each magnetic R atom has three nearest neighbors in the same double plane with parallel moments and one neighbor with opposite moment in another double plane. Each magnetic atom has six next-nearest neighbors with parallel moments and six next-nearest neighbors with opposite moments.

Following Ref. 2 we define the ferromagnetic and antiferromagnetic components as $M_F = M \sin \theta$ and $M_{AF} = M \cos \theta$, respectively, where M is the total moment and θ is the canting angle. The free energy written within the frame of Heisenberg model is given as follows:

$$E = -J_{nn}M^2(3 - \cos 2\theta) - 6J_{nnn}M^2(1 - \cos 2\theta). \quad (1)$$

Minimization of Eq. (1) gives two stable magnetic configurations: ferromagnetic (FM) ($\theta = \pi/2$) and antiferromagnetic (AFM) ($\theta = 0$). The energy of the FM state depends linearly on J_{nnn}/J_{nn} , while the energy of the AFM state does not depend on J_{nnn}/J_{nn} (Fig. 6). According to this model,

the ground state is FM when $J_{nnn}/J_{nn} > -1/6$ and is AFM otherwise.

The observed transition from a ferromagnetic to a canted antiferromagnetic structure in $\text{Er}(\text{Mn}_{0.95}\text{Al}_{0.05})_2$ suggests that in this compound the energies of the FM and AFM states are close to each other. It could be the case if J_{nnn} is negative and the ratio of J_{nnn}/J_{nn} is close to the threshold value of $-1/6$.

A negative exchange interaction between the next-nearest neighbors, resulting from the oscillating character of the RKKY interaction $J(R)$, is known in $R\text{Al}_2$ compounds. In the inset of Fig. 6 the variation of $J(R)$ in NdAl_2 calculated from inelastic neutron scattering data is shown.¹⁴ Similar results have been reported for HoAl_2 (Refs. 15 and 16). One could speculate that in $\text{Er}(\text{Mn},\text{Al})_2$ a small change of interatomic distances induced by Al substitution changes the relative magnitudes of the J_{nnn} and J_{nn} exchange interactions and consequently the energy balance between FM and AFM states.

The proposed simple model clearly shows the importance of the negative next-nearest-neighbor exchange interaction in forming of the magnetic structure in $\text{Er}(\text{Mn},\text{Al})_2$ system and can explain the appearance of antiferromagnetic components.

This model cannot be applied for the hexagonal phase which has a different symmetry from the Er environment. In the cubic phase the Er ion has point symmetry $\bar{4}3m$ while in the hexagonal phase the inversion is absent and the point group is $3m$ only. Indeed a simple antiferromagnetic structure similar to that observed in the cubic phase has not been observed in the hexagonal Laves phases. However, some hexagonal phases like PrMn_2 and NdMn_2 show complex noncollinear magnetic arrangement,¹⁷ which could be related to a negative next-nearest-neighbors R - R exchange interaction, combined with the dominant R -Mn interaction.

IV. CONCLUSION

The neutron diffraction study of the $\text{Er}(\text{Mn}_{1-x}\text{Al}_x)_2$ system shows that with increasing Al content the hexagonal $C14$ structure becomes unstable and the cubic $C15$ structure appears. The hexagonal phase, which exists at low Al content only, shows a ferromagnetic structure with very weak Mn moments. In the cubic phase at $x \leq 0.15$ long-range ferromagnetic order of Er moments with practically nonmagnetic Mn moments is observed. At higher Al content, in the region of the instability, the long-range order of the Er moments is replaced by a short-range order, which probably involves weak intrinsic Mn moments.

The presence of antiferromagnetism in the Er-Mn system, previously considered as a simple ferromagnet,¹⁸ can be qualitatively explained by taking into account the negative next-nearest-neighbor Er-Er exchange interaction J_{nnn} , together with the positive nearest-neighbor exchange interaction J_{nn} . A threshold value for the appearance of antiferromagnetism in $\text{Er}(\text{Mn},\text{Al})_2$ is expected for the ratio $J_{nnn}/J_{nn} = -1/6$.

The Mn moments remain very small and do not play any role in stabilization of the long-range magnetic order in $\text{Er}(\text{Mn},\text{Al})_2$, in contrast with $\text{Ho}(\text{Mn},\text{Al})_2$ (Ref. 3) and

Dy(Mn,Al)₂ (Ref. 2) systems, which are closer to the instability region. The *R*-Mn exchange interaction, which dominates in the last systems, is negligible in the Er compounds. In Er(Mn,Al)₂, the antiferromagnetic structure results from negative next-nearest-neighbor interactions in the Er lattice, while in Dy and Ho systems it comes from the strong negative *R*-Mn interaction.

ACKNOWLEDGMENTS

The work was supported by grants from RFBR (Nos. N-02-02-16981 and N-03-02-16482) and the Russian Federal Foundation for Neutron Studies on Condensed Matter. The authors thank Dr. S. Granovsky for help in the sample preparation and V. Konetchnyi for help in experiments.

-
- ¹M. Shiga, *J. Magn. Magn. Mater.* **129**, 17 (1994).
²I. Golosovsky, I. Mirebeau, A. Markosyan, P. Fischer, and V. Pomjakushin, *Phys. Rev. B* **65**, 014405 (2002).
³I. Golosovsky, I. Mirebeau, A. Markosyan, J. Rodriguez-Carvajal, and T. Roisnel, *J. Phys.: Condens. Matter* **36**, 11 737 (2002).
⁴G. Felcher, L. Corliss, and J. Hastings, *J. Appl. Phys.* **36**, 1001 (1965).
⁵H. Oesterreicher, *J. Phys. Chem. Solids* **33**, 1031 (1972).
⁶B. Ouladdiaf, R. Ballou, J. Deportes, and E. Lelievre-Berna, *J. Magn. Magn. Mater.* **140-144**, 1811 (1995).
⁷J. Rodriguez-Carvajal, computer code FULLPROF, LLB, Saclay, France, 2000.
⁸K. Hardman, J. Rhyne, S. Malik, and W. Wallace, *J. Appl. Phys.* **53**, 1944 (1982).
⁹C. Ritter, R. Cywinski, S. Kilcoyne, and S. Mondal, *J. Phys.: Condens. Matter* **4**, 1559 (1992).
¹⁰C. Ritter, S. Kilcoyne, and R. Cywinski, *J. Phys.: Condens. Matter* **3**, 727 (1991).
¹¹P. Brown, B. Ouladdiaf, R. Ballou, J. Deportes, and A. Markosyan, *J. Phys.: Condens. Matter* **4**, 1103 (1992).
¹²C. Ritter, R. Cywinski, S. Kilcoyne, S. Mondal, and B. Rainford, *Phys. Rev. B* **50**, 9894 (1994).
¹³C. Ritter, R. Cywinski, and S. Kilcoyne, *Z. Naturforsch., A: Phys. Sci.* **50**, 191 (1995).
¹⁴A. Furrer and H. Purwins, *Phys. Rev. B* **16**, 2131 (1977).
¹⁵W. Schelp, A. Leson, W. Drewes, H. Purwins, and H. Grimm, *Z. Phys. B: Condens. Matter* **51**, 41 (1983).
¹⁶J.J. Rhyne and N.C. Koon, *J. Magn. Magn. Mater.* **31-34**, 608 (1983).
¹⁷R. Ballou, J. Deportes, R. Lemaire, and B. Ouladdiaf, *J. Appl. Phys.* **63**, 3487 (1988).
¹⁸K.N. Taylor and M.I. Darby, *Physics of Rare Earth Solids* (Chapman and Hall, London, 1972).